Article ID: 1006-8775(2013) 01-0016-12

POSSIBLE RELATIONSHIP BETWEEN THE INTERANNUAL ANOMALY OF THE TROPICAL PACIFIC SEA SURFACE HEIGHT AND SUMMER PRECIPITATION IN CHINA

LI Li-ping (李丽平)[1], WANG Chao (王 超)[2], ZHANG Kai-mei (章开美)[3]

(1. Key Laboratory of Meteorological Disaster of Ministry of Education/Nanjing University of Information Science and Technology, Nanjing 210044 China; 2. Jiangmen Meteorological Bureau, Jiangmen, Guangdong 529030 China; 3. Jiangxi Meteorological Service Center, Nanchang 330046 China)

Abstract: By using NCEP GODAS monthly sea surface height (SSH) and 160-station monthly precipitation data in China, the seasonal and interannual characteristics of SSH are analyzed over the tropical Pacific, and correlations between SSH and summer rainfall are discussed. The results are shown as follows: (1) The tropical Pacific SSH takes on a "V" pattern in the climatic field with an eastward opening, and it is higher in the western part (in the northwestern part) than in the eastern part (in the southwestern part). The high-value areas are more stable in the northwest, and the value range (greater than 0.8 m) is larger in spring and summer than in autumn and winter. The high-value area in the southwestern part is the largest (smallest) and more northerly (southerly) in spring (summer). SSH is higher in spring and autumn than in summer and winter over the equatorial zone. (2) The interannual anomalies of the SSH are the strongest over the tropical western and southwestern Pacific and are stronger in winter and spring than in summer and autumn. The interannual anomalies are also strong over the equatorial middle and eastern Pacific. The distribution ranges are larger and the intensities are stronger in the autumn and winter. There is a close relationship between the SSH interannual anomalies and ENSO events in autumn, winter and spring. (3) When ENSO events take place in winter, according to the simultaneous relationship among the tropic Pacific SSH, 850 hPa wind fields and the summer precipitation of China, it can be predicted that the precipitation will be significantly more than normal over the south of the Yangtze River, especially over Dongting Lake and Poyang Lake region, eastern Qinghai-Tibet Plateau, Yangtze-Huai River Valley, eastern part of Inner Mongolia and less than normal over the area of Great Band of Yellow River, North China and South China in successive summers.

Key words: sea surface height; interannual anomalies; tropical Pacific Ocean; summer rainfall of China

CLC number: P426.6 **Document code:** A

1 INTRODUCTION

Sea level variation is an important scientific issue in the study of the physical oceanography and atmospheric science. Sea level, as the interface between the sea and air, is an important expression of the characteristic of the subsurface sea water and ocean circulation, which responds subtly to the climatic change[1]. The variations of the sea level have an important effect on the oceanic and atmospheric systems and everyday life. In recent years, with the rapid expansion of the influence of the human activities on the oceanic and atmospheric system, greenhouse effect is being aggravated, leading to speedy sea level rise and posing a great threat to the environment in which the human being exists. Sea level variation has become an important issue of the community concerned. Sea level changes appear at two levels, one being global and the other being regional. The major factors affecting absolute global changes in the sea level can be summarized as two aspects[2]. One is the changes of the global seawater quality, mainly including ice/snow melting and accumulation, precipitation, evaporation, surface runoff and air-land water mass exchange. The sea level variations (rise and ebb) they induce are closely

Received 2011-11-29; **Revised** 2012-12-13; **Accepted** 2013-01-15

Foundation item: Specific Project on Public Fields (GYHY201006038, GYHY201006020); "973" Program (2013CB430202, 2012CB417205); Third-level Talent Training Project of the fourth "333 project" in Jiangsu Province; a project by the Priority Academic Program Development of Jiangsu Higher Education Institutions (PAPD)

Biography: LI Li-ping, Ph.D., primarily undertaking research on regional air-sea interaction and intraseasonal oscillation.

Corresponding author: LI Li-ping, e-mail: li.liping@163.com

related to climate. The other is the changes of the seawater density, including temperature and salinity changes, which is named as specific capacity effect. The regional or local sea level changes are quite different from those of the globally mean sea level. As sea water contains strong air-sea interaction signal, the subsurface variations over the tropical Pacific play an important role in the global climate changes[3]. The sea level variations over the Pacific represent special laws and characteristics because of its unique geographical environment, air-sea interaction, the global warming and other factors. In recent years, scholars both at home and abroad have intensively researched the long-term variation trends of the sea level by using the data from tidal stations and satellite altimeters[4, 6-8]), and the results showed that the sea level of the Pacific has a tendency to ascend during the past decades and exhibits accelerated rise in the most recent decade. It exists significantly regional features for the long-term trend of the sea level[9]. The sea level over the tropical Pacific shows significantly interannual and interdecadal changes[10-12], and El Niño/Southern Oscillation (ENSO) and Pacific Decadal Oscillation (PDO) are important factors influencing these variations respectively[13]. Many investigations have observed that ENSO has obvious effects on the interannual variations of sea level over the Pacific[14, 15]. Hu and Liu[3] investigated the temporal and spatial characteristics of Sea Surface Height (SSH) over the tropical Pacific at different time scales by using satellite altimetry data. Liu and Wang[16] disclosed the spatial features of the intraseasonal oscillation of SSH over the tropical Pacific. Li et al.[17] dealt with the interdecadal characteristics of SSH over the tropical Pacific by using the SSH data of Simple Ocean Data Assimilation (SODA).

In short, there have been many research results about sea surface height over the tropical Pacific since the emergence of observations from remote-sensing satellites. However, most of the studies used short data series or only studied the sea surface height. Some researches show that the climatic evolution is of obvious interannual characteristics over the Pacific [18-20], and this kind of interannual variability is related to ENSO[21-23]. There have been many studies about the influences of ENSO-pattern sea surface temperature (SST) anomaly and atmospheric circulation anomaly on the precipitation in China[24-27]. How does the SSH, which is closely related to ENSO in the tropical Pacific, related to the summer precipitation in China? This is an issue deserving further study. This paper will study the interannually temporal and spatial characteristics of SSH over the tropical Pacific based on the National Centers for Environmental Prediction (NCEP) Global Ocean Data Assimilation System (GODAS, USA) monthly sea surface height data during the past 30 years, and further investigate its correlations with the summer precipitation in the east of China, so as to provide some references for short-term climatic prediction of the summer precipitation in China.

2 DATA AND METHODS

Data from the following sources were used in this study. First, the monthly SSH data were from NCEP GODAS[28]. The data were from the period of January 1980 to December 2009, with a horizontal resolution of 1.0°×0.333°. Second, we used the 850 hPa wind field (V_{850}) from NCEP and the National Center for Atmospheric Research (NCAR) reanalysis data from January 1951 to December 2009, with a horizontal resolution of 2.5°×2.5°[29]. Third, we used monthly precipitation data from 160 weather stations located throughout China from January 1951 to December 2009[30]. Only data collected from January 1980 to December 2009 were chosen for further analysis.

Next, harmonic analysis was performed to remove from the data oscillatory factors whose period was at or above 10 years. Hereafter, the data for spring, summer, fall and winter are defined as the means for the months of MAM, JJA, SON and DJF (of the successive year), respectively. The area (20°S to 20°N and 120°E to 60°W) was used to represent the tropical Pacific region. In addition, the empirical orthogonal function (EOF) and correlation analysis methods were used.

3 THE CLIMATIC CHARACTERISTICS OF SSH OVER THE TROPICAL PACIFIC

Chen et al.[31] pointed out that there are clear variations for SSH over the different periods in a year and different sea areas. In the Northern Hemisphere, the SSH maximum and minimum appear in September and March, respectively and the opposite is true for the Southern Hemisphere. Shen et al.[5] also got similar results. Yan and Zuo[32] discovered that the SSH is generally highest in June and July and lowest in December and January over the low latitudes (15°S to 15°N) of the tropical area. What are the seasonal characteristics of SSH in the tropical Pacific (20°S to 20°N)? It can be seen from the annual average SSH charts over the tropical Pacific in four seasons (Figure 1) that the seasonal variation range of SSH is roughly between 0.0 and 1.0 m over the tropical Pacific. In spring (Figure 1a), the high-value area (>0.6 m) exists over the tropical northwestern Pacific (north of 10°N, 120°E to 160°W) and over the southwestern Pacific (south of 5°N, 145°E to 150°W). The SSH is lower in the eastern part than in the western part of the tropical Pacific and is about 0.2 m. Compared with the SSH in spring, the range of high SSH (>0.6 m) over the tropical southwestern Pacific in summer (Figure 1b) obviously contracts to the south, and the high-value area near the equatorial (southwestern) Pacific extends to the east (contracts to the west) in autumn. The SSH features in winter are very similar to those in autumn, but it is the lowest between the equator and 10°N in the four seasons.

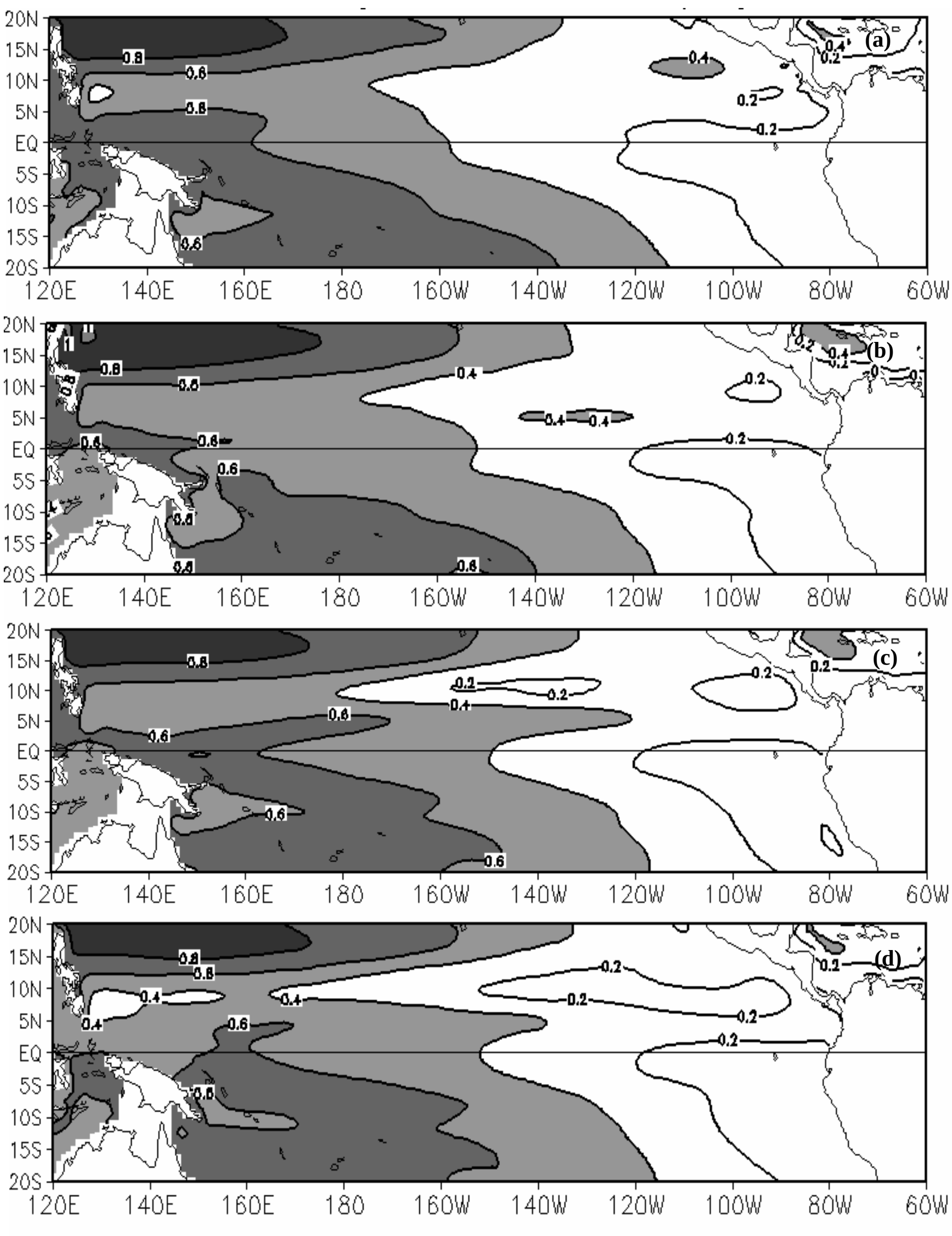

Figure 1. Climatic fields of SSH in the tropical Pacific in (a) spring, (b) summer, (c) autumn and (d) winter. Units: m; contour interval: 0.2; the shaded values>0.4.

In summary, the climatic fields of the tropical SSH exhibit an eastward-opening "V" pattern and is higher in the west (in the northwest) than in the east (southwest), which is determined by the wind stress anomalies. The intensity of the anomalous easterlies is symmetric about the equator in the tropical Pacific and gradually decreases from the equator to the mid-latitudes, resulting in the "V" pattern distribution of SSH opening eastward[5], but there are some seasonal variations for the SSH over the tropical Pacific. The high-value region is stable and moves little in the northwest and the range (SSH > 0.8 m) is a little larger in spring and summer than in autumn and winter. The high-value range in the southwest is the largest and northward in spring and the smallest in summer and southward. The range is situated between the above two conditions in autumn and winter. SSH in the equatorial regions is higher in spring and autumn than in winter and summer. The above seasonal characteristics of SSH are mainly related to SST changes (namely, the changes of specific volume) caused by the solar radiation[5, 33]. Yan and Zuo[32] discovered that the changes of specific volume are the main factors inducing the seasonal variations of SSH in the Northern Hemisphere, and it is also the factors that influence the seasonal variations of SSH in the Southern Hemisphere, but other factors play an opposite role compared to specific volume and their contributions are more significant.

In order to learn about the mean interannual intensity characteristics of SSH over the tropical Pacific in the four seasons, Figure 2 illustrates the simultaneous SSH standard deviation fields in the tropical Pacific. The interannual anomalies of SSH are large over the tropical western Pacific, tropical southwestern Pacific, tropical central Pacific and the equatorial eastern Pacific, and largest over the first two areas in spring. The SSH interannual anomalies are significant over the tropical western Pacific between 5°N and 15°N, southwest Pacific, the areas near 10°N and the central and eastern equatorial Pacific in summer. The anomalous features in autumn are similar to those in summer, but the anomalous extension is larger and the intensity is stronger, especially over the tropical west Pacific and equatorial central and eastern Pacific. The anomalous extension in winter is larger than that in autumn over the west and east of tropical Pacific, and the anomalies are stronger in the west.

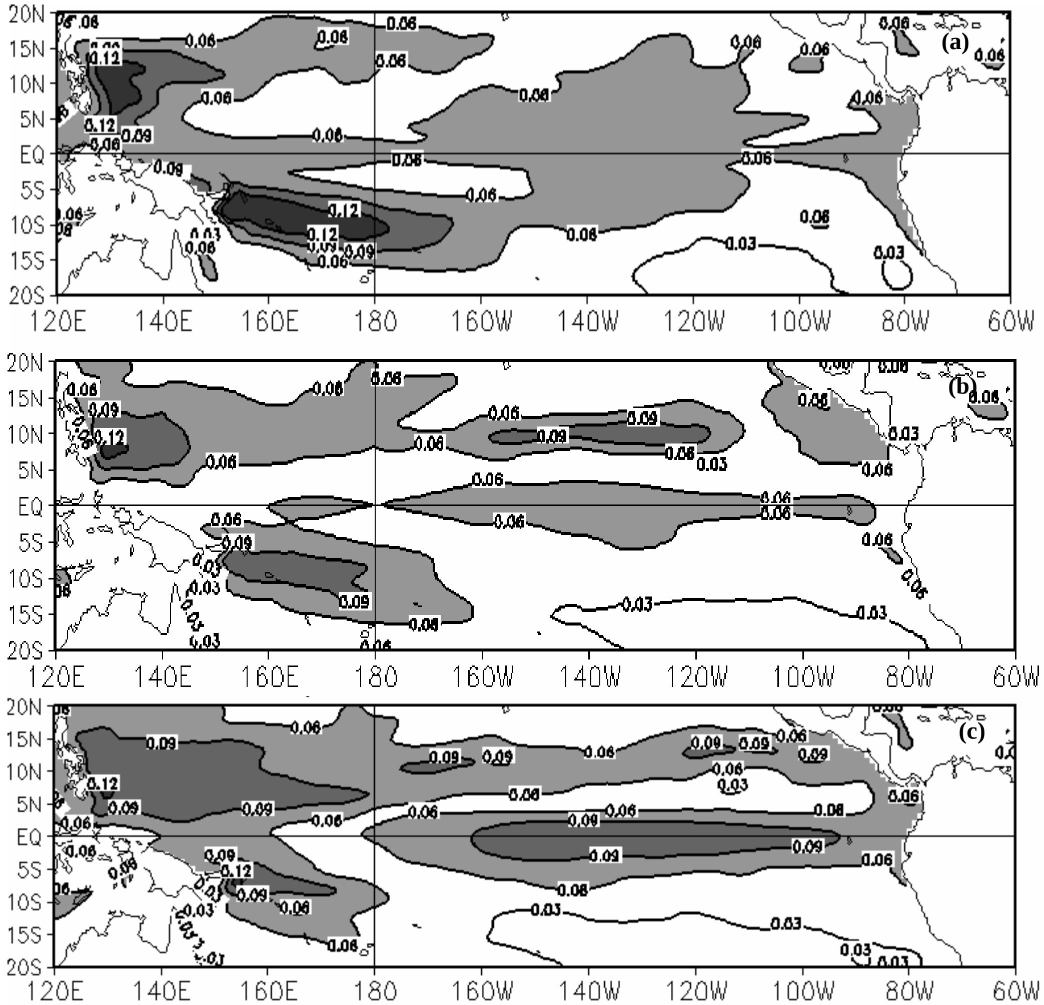

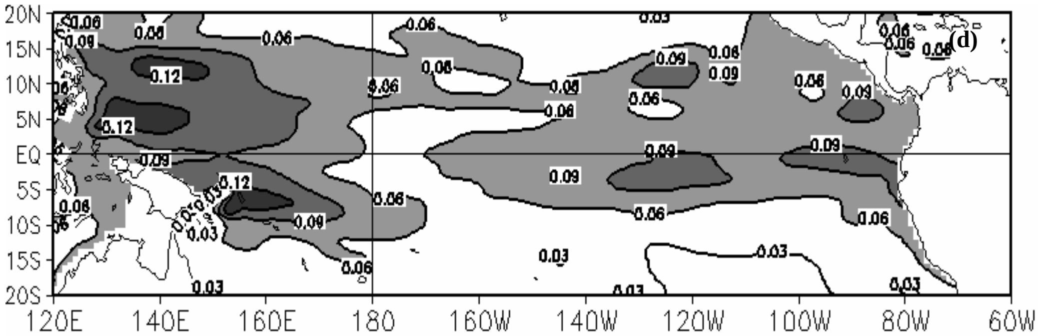

Figure 2. Standard deviation fields of SSH in the tropical Pacific in (a) spring, (b) summer, (c) autumn and (d) winter. Units: m; contour interval: 0.03; the shaded values>0.06.

In short, there are obvious differences in the annual mean interannual anomaly in terms of significant areas and intensity of SSH during different seasons. The interannual anomaly intensity is large over the tropical western Pacific and southwestern Pacific in each of the seasons and stronger in winter and spring than in summer and autumn. The interannual anomaly over the equatorial middle Pacific is also large. The intensity and extension are both large in autumn and winter. The interannual anomaly near 10°N over the tropical central and eastern Pacific is also large.

4 ANALYSIS OF SPATIOTEMPORAL CHARACTERISTICS OF SSH INTERANNUAL ANOMALIES IN THE TROPICAL PACIFIC

The spatiotemporal characteristics of SSH interannual anomalies over the tropical Pacific in spring, summer, autumn and winter are respectively investigated by using the Empirical Orthogonal Function (EOF) method. The main results are as follows.

4.1 *Analysis of variance*

The variance contribution ratios of the first 10 EOF main modes of SSH in each season are listed in Table 1. The variance contribution of the first mode in spring, autumn and winter is all more than 40% and increases in the order of season. Compared with these three seasons, the variance contribution of the first mode in summer is 31.6% and decreases remarkably. The contribution ratio of the second mode is the maximum in four seasons, which shows that the structure of SSH is the simplest in winter and the most complicated in summer. The first mode is mainly described below.

Table 1. Variance contribution ratio of EOF analysis on SSH in each season (%).

	1	2	3	4	5	6	7	8	9	10
Spring	42.4	16.7	10.7	5.5	2.7	2.5	2.3	1.9	1.8	1.6
Summer	31.6	23.2	9.6	5.7	4.7	3.2	2.7	2.2	1.9	1.8
Autumn	54.7	15.5	4.2	3.9	3.0	2.7	1.8	1.7	1.4	1.4
Winter	58.4	10.7	5.0	3.7	3.1	2.4	2.2	2.1	1.5	1.4

4.2 *The interannual spatiotemporal characteristics of SSH anomalies*

The time series of the SSH first mode in autumn, winter and spring are closely related to El Niño/La Niña events (Figures 3b, .4b, 5b, and 6b), respectively. Recent studies have shown that the SSH interannual anomalies are in close relation to the occurring and developing of ENSO[10-15]. According to the laws of ENSO development—it mostly begins in autumn, comes to maturity in winter, weakens and ends in spring, the interannual temporal and spatial characteristics of SSH anomalies are described in the order of autumn, winter, spring and summer so as to further understand their relationships with the genesis and development of ENSO.

The time coefficient series of the first EOF mode of SSH in autumn is closely connected with El Niño/La Niña events (Figure 3b). Ten El Niño events are corresponding to the peaks of the time series and seven La Nina events to the valleys. Based on the first eigenvector field (Figure 3a), it can be concluded that SSH fields over the equatorial central and eastern Pacific (inclining to the Southern Hemisphere) and the eastern Pacific (north of 10°N) exhibit positive anomalies (Figure 3a). Conversely, the tropical northwest and southwest Pacific is in negative anomalies, and the negative anomaly center lies in the western Pacific warming pool. These significant interannual anomaly regions were consistent with those of the annual average interannual anomalies (Figure 2c). By combining the time coefficient series and the eigenvector, it can be seen that when the El

Niño/La Niña event is developing, the SSH in the tropical western Pacific is negatively (positively) anomalous, but positively (negatively) anomalous in the tropical central and eastern Pacific and the eastern Pacific (north of 10°N).

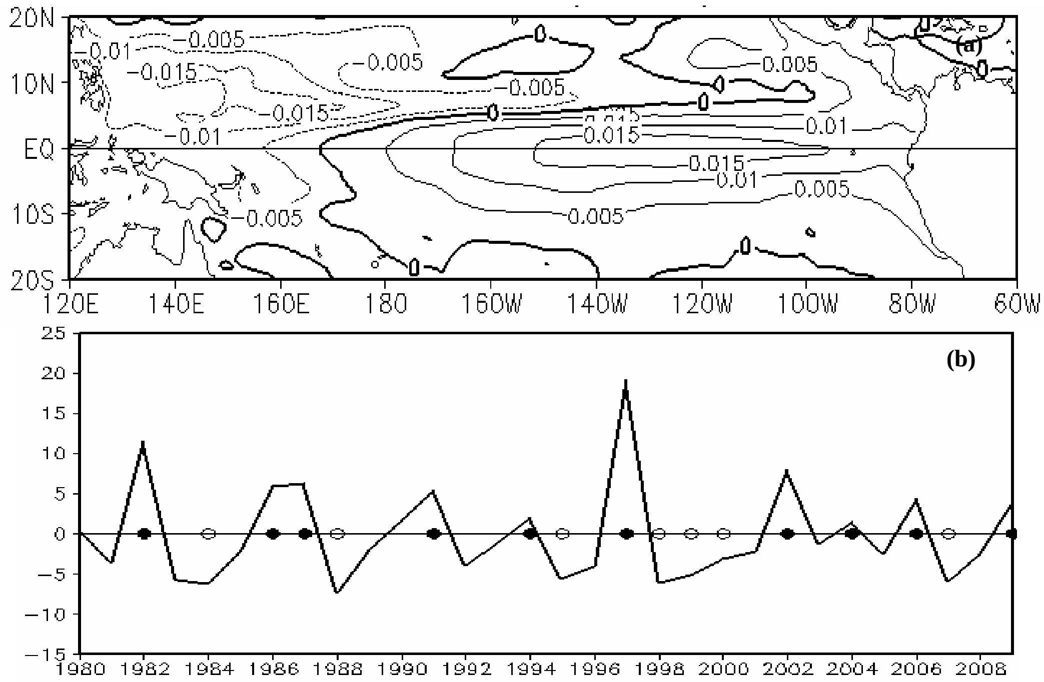

Figure 3. The EOF (a) first eigenvector (units: m; contour interval: 0.005) and (b) time coefficient (●: El Niño events; ○: La Niña events) of SSH anomalous fields in the tropical Pacific in autumn.

It is clear from the time coefficient series of the first EOF mode of the SSH in winter (Figure 4b) that nine warming events are corresponding to the peaks and seven out of eight cold events are corresponding to the valleys. The first eigenvector field (Figure 4a) shows that the tropical central and eastern Pacific exhibits positive anomalies. Conversely, the tropical northwest and southwest Pacific exhibits negative anomalies. These regions of significantly interannual anomalies are consistent with those of the annual average interannual anomalies (Figure 2d). Compared with the eigenvector in autumn (Figure 3a), the positively anomalous area over the eastern Pacific near 10°N extends to the central Pacific and the negatively anomalous area extends eastward. The ENSO event is usually in the stage of maturation in winter, making the SSH positively (negatively) anomalous in the tropical central and eastern Pacific and negatively (positively) anomalous in the tropical northwest and southwest Pacific when the El Niño (La Niña) is in the stage of maturation.

Four warming events are corresponding to the peaks and eight cooling events to the valleys of the time coefficient series of the first EOF mode of the SSH in spring (Figure 5). Combinations of time coefficient series with eigenvectors (Figure 5a) show that SSH anomalies during El Niño (La Niña) events in spring are similar to those in winter. However, the range of positive (negative) anomaly (north of 5°N) extends more westward in spring than in winter. The regions of negative (positive) anomaly south of the equator expand eastward. Overall, the large anomaly areas are corresponding to the annual average anomaly (Figure 2a). ENSO events generally begin to weaken in spring. From winter to spring, the SSH increases from east to west, reflecting the features of climatic fields.

It can be seen from Table 1 that the ratios of variance contribution of the first and second modes of SSH are bigger in summer. The significance of the two modes are tested by the use of the “North rule”[34] and are statistically significant, which indicates that the SSH anomaly tends to be complicated and there are two main patterns.

The time coefficient series of the first SSH mode in summer show interannual anomalies evidently (Figure 6b), though being basically unrelated to the ENSO event. The correlation coefficient is –0.164 between the regionally averaged SSH anomaly and the Niño3 index in summer. Therefore, SST anomaly in the Niño3 region is not the main signal determining the SSH anomaly in summer, because the ENSO signal in the Niño3 region is very weak or decreases gradually. The correlation coefficient of the EOF’s first time coefficient series between the previous winter (Figure 4b) and summer (Figure 6b) is 0.7 (being above the 99% confidence level), which indicates that this mode can reflect SSH anomalies during years of ENSO attenuation. Combinations of eigenvectors (Figure 6a) with the time coefficient series (Figure 6b) and comparisons of them with Figure 5 show that when the time coefficient is positive, the positively anomalous region north of 5°N moves westward so that the whole tropical Pacific north of 5°N is positively anomalous from spring to summer. The negative anomaly moves eastward near the equator and southward, resulting in negative SSH anomaly in the whole equatorial Pacific and to the west of 120°W.

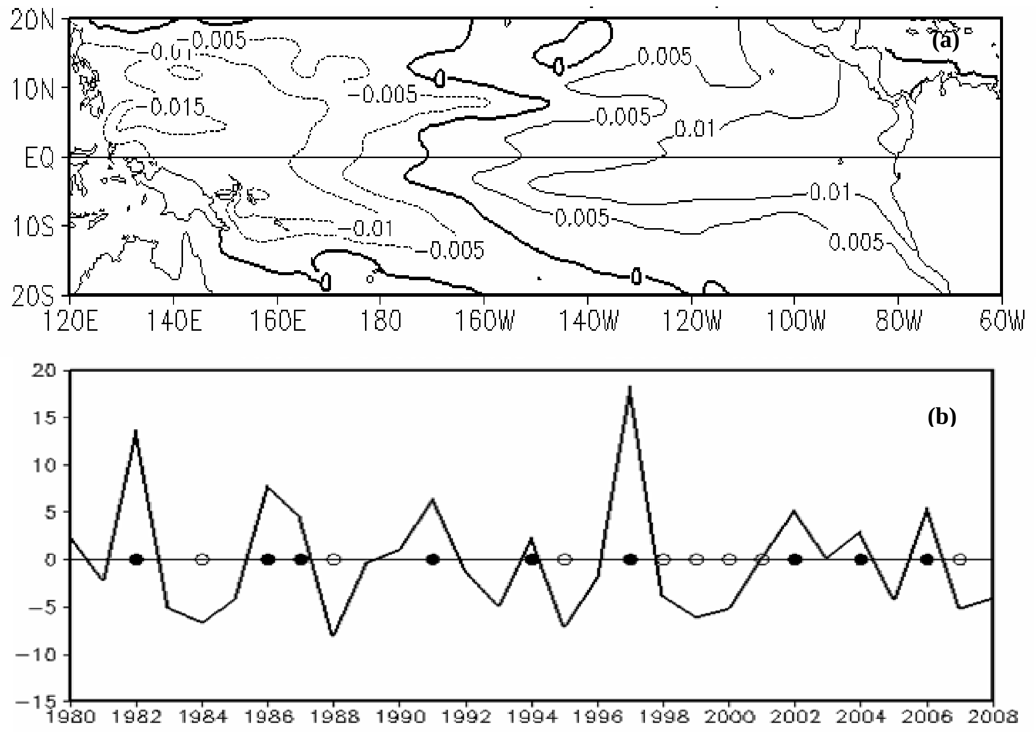

Figure 4. Same as Figure 3 but for the winter.

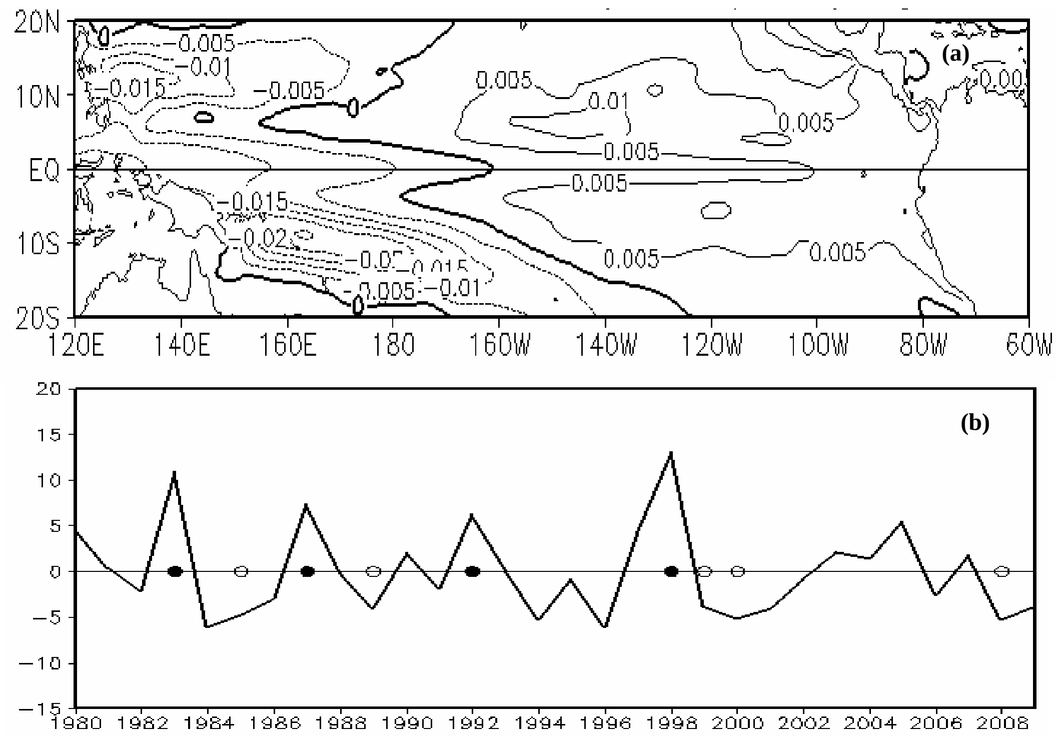

Figure 5. Same as Figure 3 but for the spring.

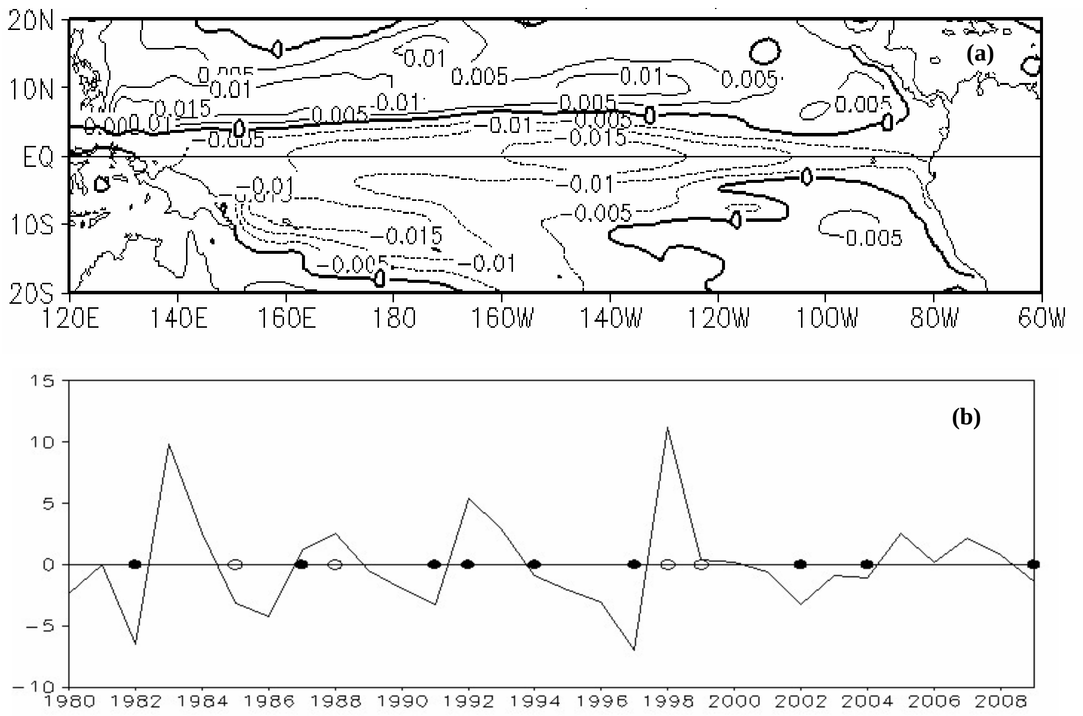

Figure 6. Same as Figure 3 but for the summer.

In addition, the second eigenvector is the El Niño pattern (figure omitted) and its time coefficient series is closely connected with the ENSO event (with the time coefficient series being positive for eight out of 10 El Niño events and negative for all of the three La Niña events). The correlation coefficient between the SSH anomaly in summer and the Niño3 index in winter is 0.682. It further shows that the ENSO is somewhat related to the SSH anomaly in summer but in a secondary position (in the form of the second mode), and the first mode, which is unrelated to ENSO, dominates in summer.

In summary, the SSH anomalies in autumn, winter and spring are closely associated with the ENSO. The SSH is positively anomalous in the tropical Pacific and negatively anomalous in the northwest and southwest Pacific during warming events. During the emergence, development, decay and disappearance of ENSO events from autumn through winter and spring to summer, the positive anomaly of the region north of 5°N extends westward while the negative anomaly near the equator and in the southwest Pacific extends eastward. The SSH anomaly in summer can well reflect the SSH situation during the attenuation and even the extinction of the ENSO event. According to the second cause which leads to the SSH anomaly[2], it is shown that the SSH interannual anomalies are related to zonal wind stress and SST anomalies during the occurrence and development of ENSO events. During the development, the westerly wind anomalies occur in the tropical western Pacific and the trade wind over the tropical Pacific is weakened substantially. The warmed water is transferred eastward by the anomalous westerly from the tropical western Pacific, resulting in decreased local SST. The weakened trade wind also inhibits the upward flow of the equatorial eastern Pacific cold water, leading to positive (negative) SST anomalies over the tropical central and eastern Pacific (the tropical western Pacific). Because of the expansion with heated sea water and the contraction with cooled sea water, positive (negative) SSH anomaly is induced.

5 POSSIBLE INFLUENCE OF SEA SURFACE HEIGHT ANOMALIES ON SUMMER PRECIPITATION IN CHINA

The literatures point out that the interannual variability of SST over the Pacific is closely associated with ENSO in the Pacific[18-20] and has a significant effect on the monsoon and precipitation[24]. The above analysis shows that the SSH interannual anomalies in the tropical Pacific are also related to ENSO, then what relationships are there in the interannual anomalies between SSH and summer rainfall in China, and what are the characteristics for the corresponding circulation anomalous? The following section attempts to probe into the direct interannual anomalies relationships between SSH and summer precipitation in China, and also indirectly studies the relationships of ENSO with China's summer precipitation by analyzing their time-lagged and simultaneous correlations. The anomalous characteristics of corresponding circulation are further analyzed. These are done in an attempt to summarize the oceanic and atmospheric signals that predict the summer rainfall in China.

5.1 *The time-lagged and simultaneous correlations between SSH and the summer rainfall anomalies in China*

Figures 7a to 7d illustrate the time-lagged (simultaneous) correlations between the time coefficient series for the first EOF mode of SSH anomaly over the tropical Pacific in the preceding autumn, winter and spring (summer) and the summer rainfall in China, respectively. It can be seen that the distributions of positive and negative correlation are similar to those between the SSH anomalies in the preceding autumn and winter and the summer rainfall in China. Positive correlations are found in the Sichuan Basin, the reaches of Hanshui River, the middle and lower reaches of Changjiang-Huaihe Rivers Basin, the eastern Inner Mongolia and northern Xinjiang. Negative correlations are presented in Yunnan, southern China, north China and three northeastern provinces. The zones of significant correlation mainly lie in the reaches of Hanshui River, the eastern Inner Mongolia, southern Yunnan and northwest Xinjiang, and the northern Xinjiang and northwest Gansu are also significant positive-correlation zones in the preceding winter. The correlation pattern in spring (Figure 7c) is similar to those in the previous autumn and winter, but the area of significant positive correlation is somewhat smaller than in the previous winter. The significantly correlated regions obviously increase in summer (Figure 7d) and mainly lie in the Dongting Lake and the Poyang Lake basins, the eastern Inner Mongolia, northern Xinjiang and eastern Qinghai-Tibetan Plateau. According to the previous section, the SSH anomaly in summer basically reflects the anomalous conditions during the period of the attenuation and extinction and is well correlated with China's summer precipitation simultaneously. Therefore, when the ENSO event occurs in the previous winter, the summer precipitation in China can be predicted using this relationship.

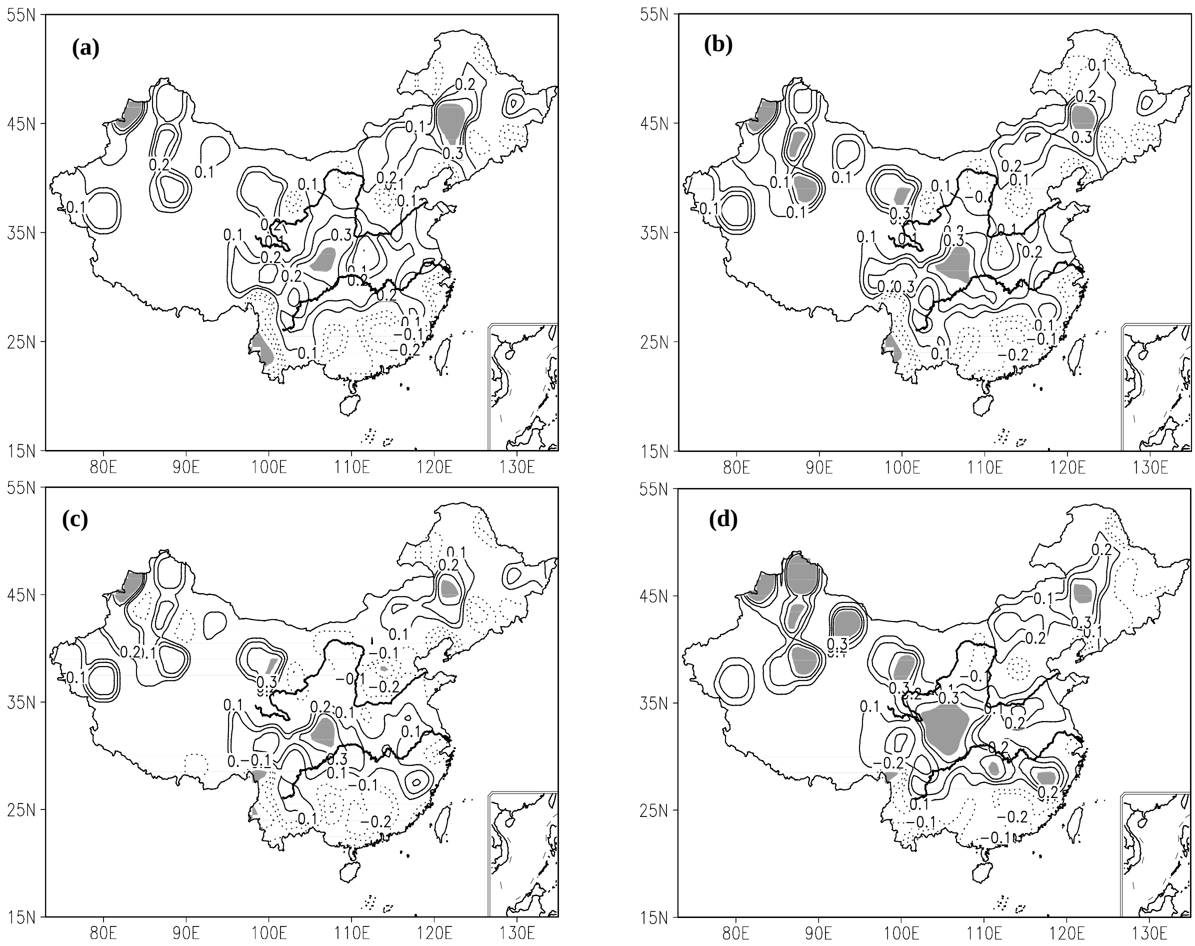

Figure 7. Time-lagged and simultaneous correlation coefficients between the first time coefficient series of EOF fro SSH anomalies in (a) autumn, (b) the preceding winter, (c) spring and (d) concurrent summer and the summer precipitation anomalies, respectively. The shaded areas are significant at the α=0.05 level.

5.2 *The correlation relationships between SSH and the 850 hPa wind fields in summer*

Due to the air-sea interaction, the tropical SSH anomalies cause atmospheric circulation anomalies. In order to learn about the relationship between these two parameters, linear regression coefficients of the EOF first time coefficient series of the summer tropical SSH anomaly on 850 hPa summer wind fields (Figure 8) are calculated by using the linear regression of variable analysis. It can be seen that anti-cyclonic circulation is produced over the eastern Asian coast, South China Sea and the sea east of Taiwan, while a strong cyclonic circulation anomaly controls the air over the Japanese archipelago. In the high latitudes, cyclonic circulation hovers above Lake Baikal and anti-cyclonic circulation covers the Kuril Islands. Consequently, a phase-locked arrangement develops between two Rossby wave trains, which are located in the northeast of the warm pool regions and mid-latitude areas, respectively. It is beneficial for the southward shift, westward expansion, and strengthening of the subtropical high in the western Pacific. Subsequently, northerly airflows at the western end of the cyclonic circulation around Lake Baikal transports cold air southward from the north, and the cyclonic circulation above the Japanese archipelago propels cold and moist airflows southward from the northeast in the mid-latitude area. In the Yangtze-Huaihe River Basin, these cold airflows meet with rich water vapor from the west end of a subtropical high originating from the Bay of Bengal and the Philippine Islands, resulting in abundant precipitation in this area.

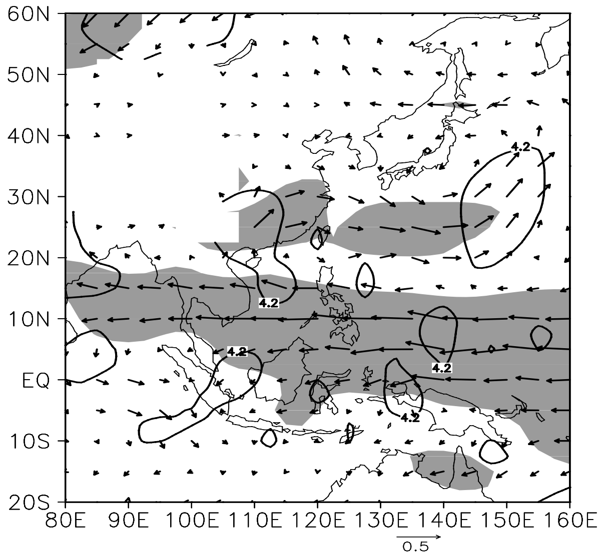

Figure 8. The coefficients in the linear regression of one variable between SSH and $\boldsymbol{V}_{850}$ (units: m/s) anomaly. Shaded (solid lines) areas are significant at the α=0.05 level for zonal (meridional) wind fields.

In summary, when El Niño-type anomalies of SSH in the tropical Pacific emerge, weaken, and gradually disappear from the preceding winter to summer, they have a long-lasting effect on atmospheric circulation in the concurrent and subsequent period. It results in a stronger subtropical high and a more westward and southward position than normal in summer. Thus, in the Yangtze-Huaihe River Basin a warm and moist southwest flow at the western end interacts with northerly cold air originating from the high-latitude Lake Baikal and northeast cold and moist air originating from the mid-latitude Japanese archipelago. Consequently, the Yangtze-Huaihe River Basin experiences increased rainfall.

6 CONCLUSIONS AND DISCUSSION

Based on an analysis of climatic characteristics of SSH in four seasons in the tropical Pacific, this paper examined the temporal and spatial properties of its interannual anomalies. Subsequently, the correlations among SSH anomalies in the tropical Pacific, the corresponding atmospheric circulation anomalies in eastern Asia, and China's summer rainfall are evaluated. The following conclusions are drawn from this analysis.

(1) The climatic fields of SSH exhibits a "V" pattern that opens eastward in the tropical Pacific, with higher values in the west (in the northwest) and lower values in the east (southwest), which is determined by the spatial distribution of wind stress anomalies. Besides, there are some seasonal variations. The high-value regions in the northwest are stable and move little. The ranges in which SSH values are greater than 0.8 m in spring and summer and are larger than those in autumn and winter. The high-value range in the southwest is the largest and northward in spring and the smallest and southward in summer, and is situated in between in autumn and winter. SSH in the equatorial region is higher in spring and autumn than in winter and summer, which is related to SST changes caused by the solar radiation.

(2) The significant areas and intensity of the annual mean interannual anomalies are obviously different for different season. In summary, the interannual anomaly intensity is large over the tropical west Pacific and southwest Pacific, and stronger in winter and spring than in summer and autumn. The interannual anomalies over the equatorial Pacific are also larger and both the intensity and the extension are larger in autumn and winter. The interannual anomalies of SSH in autumn, winter and spring are closely associated with ENSO and related to zonal wind stress and SST anomalies during the occurrence and development of ENSO events.

(3) There are close relationships among the ENSO event, SSH anomalies and atmospheric circulation anomalies. Their relationships are closer when the ENSO event is during the mature period in winter, which allows us to predict the summer precipitation in China in the year that follows. The relationship among the ENSO event, SSH anomalies, atmospheric circulation anomalies and China's summer precipitation can be described by a schematic diagram (Figure 9). Specifically, the SSH anomalies are significantly correlated with ENSO, according to the EOF time coefficient series in winter, and the correlation coefficient is 0.7 (significant at the 5% level) between the time coefficient series of EOF in winter and the subsequent summer. From section 5, it can be seen that the correlation is largest between SSH anomalies in summer and simultaneous precipitation anomalies in China. Then we make estimates as follows. When the ENSO event is at the mature phase in winter, it is predicted that precipitation will increase south of the Yangtze River, especially in the Dongting Lake Basin and the Poyang Lake Basin, the eastern Inner Mongolia, northern Xinjiang and eastern Qinghai-Tibetan Plateau, and decrease in the Great Band area of Yellow River, north of China and south of China.

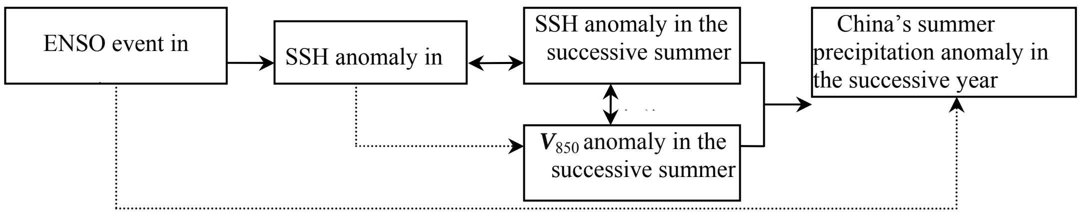

Figure 9. Diagram of the relationship among ENSO events, SSH, $\boldsymbol{V}_{850}$ and the summer precipitation in China.

It is worth noting that there are many factors affecting the SSH variations[2], and the variation of sea temperature is only one of them. There are also many factors which affect the summer precipitation in China. This paper just discloses the fact that there are close relationships between SSH and summer precipitation in China on the premise of ENSO occurrence. The ENSO event can be considered a preceding signal for predicting subsequent summer precipitation in China, and the prediction should be based on the simultaneous correlation among SSH anomaly, atmospheric circulation anomaly and China's summer precipitation anomaly.

REFERENCES:

[1] YAN Mei, ZUO Jun-cheng, FU Shen-bo, et al. Advances on sea level variation research in global and China sea [J]. Marine Environ. Sci., 2008, 27(2): 197-200.
[2] STEWART R W, BORNHOLD B D, DRAGERT H, et al. Relative sea-level change in brink [C]// The Sea, BRINK K H, ROBINSON A R, 1998, 10: 191-211.
[3] HU Rui-jin, LIU Qin-yu. Annual and intraseasonal variations in sea surface height over the tropical Pacific [J]. Oceanol. Limnol. Sinica, 2002, 33(3): 303-313.
[4] CHURCH J A, GREGORY J M, HUYBRECHTS P, et al. Changes in sea level [C] // Climate Change: the Scientific Basis. Contribution of Working Group I to the Third Assessment Report of the Intergovernmental Panel on Climate Change. Cambridge: Cambridge Univ. Press, 2001.
[5] SHEN Hui, GUO Pei-fang, QIAN Cheng-Chun, et al. Sea surface level variations during 1993-2001[J]. Oceanol. Limnol. Sinica, 2003, 34(2): 169-178.
[6] CAZENAVE A, NEREM R S. Present-day sea level change: observations and causes [J]. Rev. Geophys., 2004: 42, doi: 10.1029/2003RG000139.
[7] ANTONOV J, LEVITUS S, BOYER T P. Thermosteric sea level rise: 1955-2003 [J]. Geophys. Res. Lett., 2005, 32, doi:101.1029/2005GL023112.
[8] LOMBARD A, CAZENAVE A, LETRAON P Y, et al. Contribution of thermal expansion to present-day sea level rise revisited [J]. Global Planet and Change, 2005, 47: 1-16.
[9] CABANES C, CAZENAVE A, LEPROVOST C. Sea level rise during past 40 years determined from satellite and in situ Observations [J]. Science, 2001, 294(5543): 840-842.
[10] YOSHI N S, SHOSHIRO M, NIKLAS S, et al. Decadal sea level variability in the south Pacific in a global eddy–resolving ocean model hindcast [J]. J. Phys. Oceanogr., 2008, 38: 1731-1746.
[11] HAN W, WEBSTER P J. Forcing mechanisms of sea-level interannual variability in the Bay of Bengal [J]. J. Phys. Oceanogr., 2002, 32: 216-239.
[12] SMITH T M. Tropical Pacific sea level variations (1948-1998) [J]. J. Climate, 2000, 13(15): 2757-2769.
[13] TIWARIA V M, CABABNESB C, DOMINHB K, et al. Correlation of interannual sea level variations in the Indian Ocean from Topex/Poseidon altimetry, temperature data and tide gauges with ENSO [J]. Global and Planetary Change, 2004, 43: 183-196.
[14] GU Xiao-li, LI Pei-liang. Pacific sea level variations and their factors [J]. Acta Oceanol. Sinica, 2009, 31(1): 28-36.
[15] DONG Xiao-jun, HUANG Cheng. Monitoring global mean sea level variation with TOPEX/Poseidon altimetry [J]. Acta Geodaet. Cartograph. Sinica, 2000, 29(3): 266-272.
[16] LIU Qin-yu, WANG Qi. Spatial distribution of the sea surface height intraseasonal oscillation in the Tropical Pacific [J]. J. Ocean Univ. Qingdao, 1999, 29(4): 549-555.
[17] LI Shu-jiang, ZHAO Jin-ping, LI Yi-zhen, et al. Study on decadal variability of sea surface height in the tropical Pacific ocean [J]. Adv. Marine Sci., 2008, 26(2): 163-170.
[18] ALBERT M M, ARTHUR J M. Interdecadal variability and climate change in the eastern tropical Pacific: A review [J]. Prog. Oceanogr., 2006, 69: 267-284.
[19] WU L, LIU Z, GALLIMORE R, et al. Pacific decadal variability: the tropical Pacific mode and the North Pacific

mode [J]. J. Climate, 2003, 16(8): 1101-1120.
[20] DANIEL M W, THOMSON R E. Interannual to multidecadal timescale climate variations in the northeast Pacific [J]. J. Climate, 2000, 13(18): 3209-3220.
[21] RONG Zeng-rui, LIU Yu-guang, CHEN Man-chun, et al. Mean sea level change in the global ocean and the South China Sea and its response to ENSO [J]. Marine Sci. Bull., 2008, 27(1): 1-81.
[22] LI Chong-yin, ZHU Jin-hong, SUN Zhao-bo. The study interdecadel climate variation [J]. Clim. Environ. Res., 2002, 7(2): 209-218.
[23] MO Ru-ping. Interannual oscillation of precipitation and temperature in China and its relationships with ENSO [J]. Acta Oceanol. Sinica, 1989, 11(2): 16-41.
[24] YANG Xiu-qun, ZHU Yi-min, Xie Qian, et al. Advances in studies of Pacific decadal oscillation [J]. Chin. J. Atmos. Sci., 2004, 28(6): 1-5.
[25] LIN Xue-chun, YU Shu-qiu. El Nino and rainfall during the flood season (June-August) in China [J]. Acta Meteor. Sinica, 1993, 51(4): 434-441.
[26] YANG Xia, GUAN Zhao-yong, ZHU Bao-lin. Role of Indian Ocean dipole events in the influence of ENSO on the summer rainfall and temperature in China [J]. J. Nanjing Inst. Meteor., 2007, 30(2): 170-177.
[27] ZHU Yi-min, YANG Xiu-qun, CHEN Xiao-ying, et al. Interdecadal variation of the relationship between ENSO and summer interannual climate variability in China [J]. J. Trop. Meteor., 2007, 23(2): 105-116.
[28] BEHRINGER D W, XUE Y. Evaluation of the global ocean data assimilation system at NCEP: The Pacific ocean [C]// Preprints, Eighth Symposium on Integrated Observing and Assimilation Systems for Atmosphere, Oceans, and Land Surface, Amer. Meteor. Soc., Settle, 2004: 2.3.
[29] KISTLER R, E KALNAY, W COLLINS, et al. The NCEP-NCAR 50-year reanalysis: Monthly neans CD-ROM and documentation [J]. Bull. Amer. Meteor. Soc., 1999: 82, 247-267.
[30] National Climate Center. Monitoring and Diagnosis Data [EB/OL]. http://ncc.cma.gov.cn/cn/member.php?Login=1.
[31] CHEN J L, WILSON C R, CHAMBERS D P, et al. Seasonal global water mass budget and mean sea level variations [J]. Geophys. Res. Lett., 1998, 25(19): 3555-3558.
[32] YAN Mei, ZUO Jun-cheng. The study of thermodynamic mechanism of global sea level variation [D]. Theses for Doctoral Degree, Qingdao: Ocean University of China, 2008.
[33] CHEN J L, WILSON C R, TAPLEY B D, et al. Contributions of hydrological processes to sea level change [J]. Physics and Chemistry of the Earth, Part A/B/C, 2002, 27(32-34): 1439-1443.
[34] WEI Feng-ying. Modern Climatic Statistical Diagnosis and Prediction Technology [M]. Beijing: China Meteorological Press, 2007: 110-111.

Citation: LI Li-ping, WANG Chao and ZHANG Kai-mei. Possible relationship between the interannual anomaly of the tropical Pacific sea surface height and summer precipitation in China. *J. Trop. Meteor.*, 2013, 19(1): 16-27.